



## Development of optimal diaphragm-based pulsation damper structure for high-pressure GDI pump systems through design of experiments

Juyeong Kim<sup>a</sup>, Gil Ho Yoon<sup>b,\*</sup>, Jinyee Noh<sup>a</sup>, Jongwook Lee<sup>a</sup>, Kyungnam Kim<sup>c</sup>, Hyoungjong Park<sup>c</sup>, Jaekeun Hwang<sup>c</sup>, Yeonhong Lee<sup>c</sup>

<sup>a</sup> School of Mechanical Engineering, Kyungpook National University, 80 Sangyeok 3-dong, Buk-gu, Daegu 702-701, Republic of Korea

<sup>b</sup> School of Mechanical Engineering, Hanyang University, 222 Wangsimni-ro, Seongdong-gu, Seoul 133-791, Republic of Korea

<sup>c</sup> Motonic Corporation, 1095-11 Shindang-dong, Dalseo-gu, Daegu 704-920, Republic of Korea

### ARTICLE INFO

#### Article history:

Received 14 February 2012

Accepted 1 February 2013

Available online 5 March 2013

#### Keywords:

Pulsation damper

Pressure pulsation

Finite element procedure

Design of experiments

### ABSTRACT

This study optimizes the profile of the diaphragms of the pressure pulsation damper structure in a high-pressure GDI pump system that is now under development by applying the design of experiments (DOE) method. Because a high-pressure pulsation ranging from 0 to 10 bar reduces the performance of a GDI engine and harms it from a structural point of view, attenuating the large amplitude of the fluid pulsation pressure of the gasoline fuel injected into a GDI pump is necessary. Both the relatively low frequency range of the pressure pulsation, i.e., from 0 Hz to 30 Hz, inside the GDI engine and the high pressure of the utilized gasoline fuel prevent us from applying the existing pressure pulsation dampers such as a T-filter and Helmholtz resonator. Therefore, automotive companies utilize a new pressure pulsation damper structure called an accumulator, which is filled with gas. In the development of this pressure accumulator, it is crucial to design optimal profiles for the enveloping diaphragms in terms of the pulsation efficiency and mechanical stress for the sake of safety. In order to optimize the profile of the diaphragms used in the accumulator developed for a GDI engine, this research develops a new finite element procedure that considers the pressure variation by assuming the isoenthalpy state of the enveloped gas inside the accumulator. The developed finite element procedure is then integrated with the DOE method to determine the optimal profile for the enveloping structure of the developed accumulator. To validate the performance of the developed accumulator, the optimized accumulator is manufactured and tested.

© 2013 Elsevier Ltd. All rights reserved.

### 1. Introduction

In this research, we develop an optimal pulsation damper consisting of two metal diaphragms via the design of experiments (DOEs) method and present a finite element (FE) procedure to predict the performance of the pulsation damper according to a simplified fluid–gas–structure interaction phenomenon. Because of the inherent power and fuel efficiency advantages of a gasoline direct injection (GDI) engine, an engine with the proposed damper is considered to be an alternative for replacing the conventional multi-point fuel injection (MPFI) combustion engine [1–4]. One major difference between the GDI engine and the common MPFI engine is that gasoline is directly injected into the combustion chambers in the GDI engine to quickly and effectively mix the fuel with air. Thus, the pressure of the gasoline in both the combustion chambers and the auxiliary pipes or rails attached to the chambers of the GDI en-

gine is usually much higher than that of a normal MPFI combustion engine [1]. Naturally, this high fuel pressure induces vibrations as well as acoustic noise in the components of the GDI engine, which makes the design of more reliable components necessary from a structural safety point of view. Furthermore, the high-pressure gasoline of a GDI engine generates high fluid pressure oscillations, which are sometimes called pressure fluctuations, pressure oscillations, or pressure pulsations, during the normal or idle operations of a GDI engine, as shown in Fig. 1b. One automobile manufacturer has stated that high-pressure gasoline oscillation is not recommended because fuel oscillation directly influences the fuel efficiency of a GDI engine. Thus, it is common to install dampers called diaphragm-based pulsation dampers to reduce these observed pressure oscillations, as shown in Fig. 1. These dampers are also called pulsation dampers, resonators, or accumulators. In the present paper, we present a new FE analysis procedure based on fluid–gas–structure interaction and apply a DOE approach to determine an optimal diaphragm profile and rigorously predict and optimize the performance of a diaphragm-based pulsation damper.

\* Corresponding author. Tel.: +82 2 2220 0451.

E-mail addresses: [ghy@hanyang.ac.kr](mailto:ghy@hanyang.ac.kr), [gilho.yoon@gmail.com](mailto:gilho.yoon@gmail.com) (G.H. Yoon).

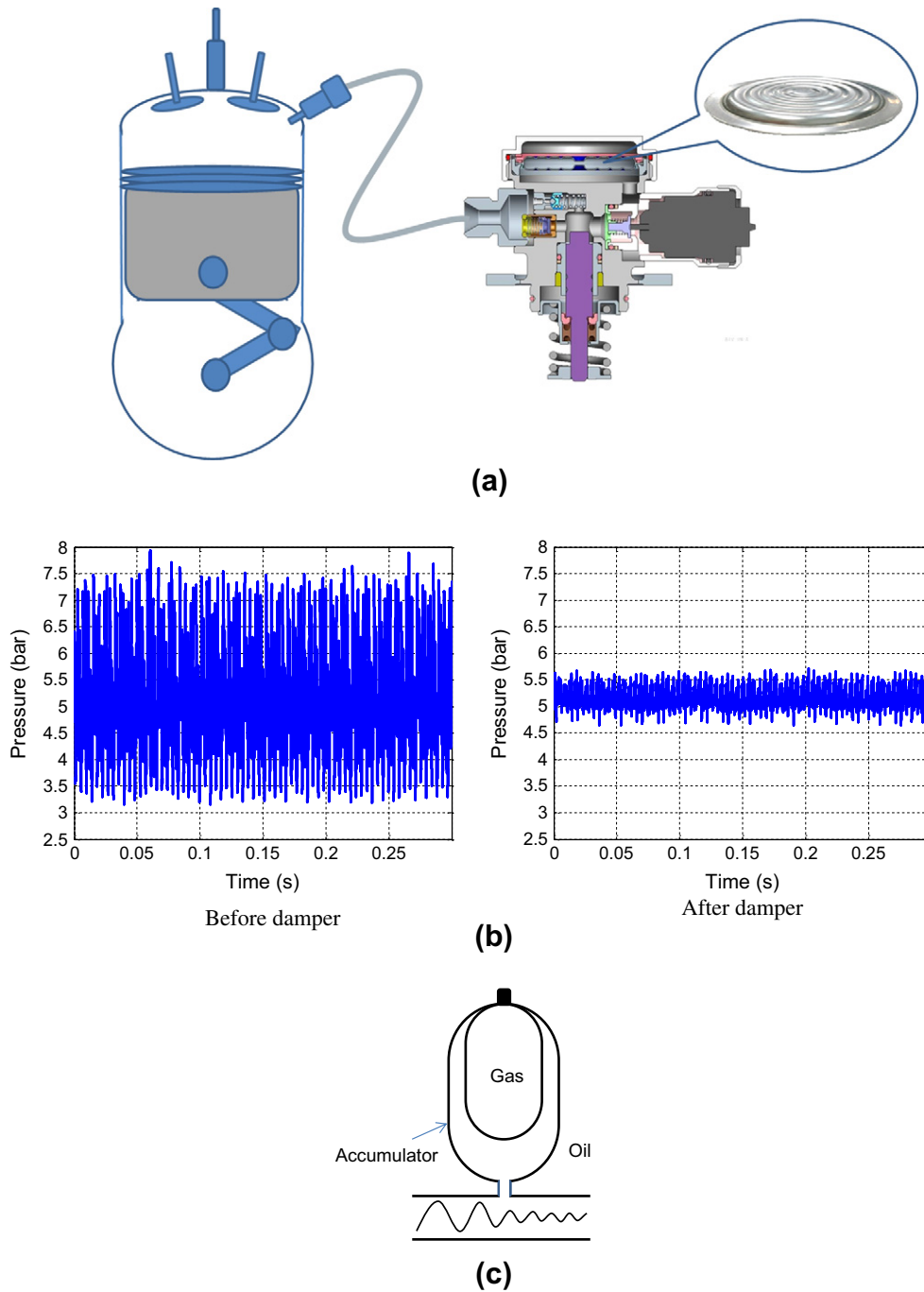


**Fig. 1.** (a) Schematic diagram of GDI engine and diaphragm-based pulsation damper, (b) typical pressure fluctuation measured in component of GDI pump (Motonic, Inc.), and (c) diaphragm-based pulsation damper [5,6].

There are many kinds of pressure or acoustic dampers [5,7–9], and many kinds of passive and active dampers have been developed [5,7,8,10] (see the Appendix A for the commonly implemented passive pulsation dampers [5,6,11–15]). Fig. 1c shows a schematic of a pulsation damper that has been commercialized for general purposes but is not suitable for automobile applications in its present form [11]. Because the separator between the gas and fluid is made of an elastic membrane such as rubber or plastic, the stiffness and strength of the diaphragm are too low to resist the high fluid pressure (around 10 bar) inside a GDI engine. With some changes, the pulsation damper under development, shown in

Fig. 1c, may be a feasible solution. The present research has the objectives of developing a systematic engineering process to calculate the performance of the new pulsation damper numerically, identifying the optimal characteristics for the pulsation damper, and verifying its performance experimentally.

The organization of this paper is as follows. In Section 2, we investigate the numerical calculation of the performance of the pulsation damper using FEM. In Section 3, we optimize the shape of the diaphragms used in the pulsation damper by applying the DOE method. In Section 4, we verify the performance of the pulsation damper.

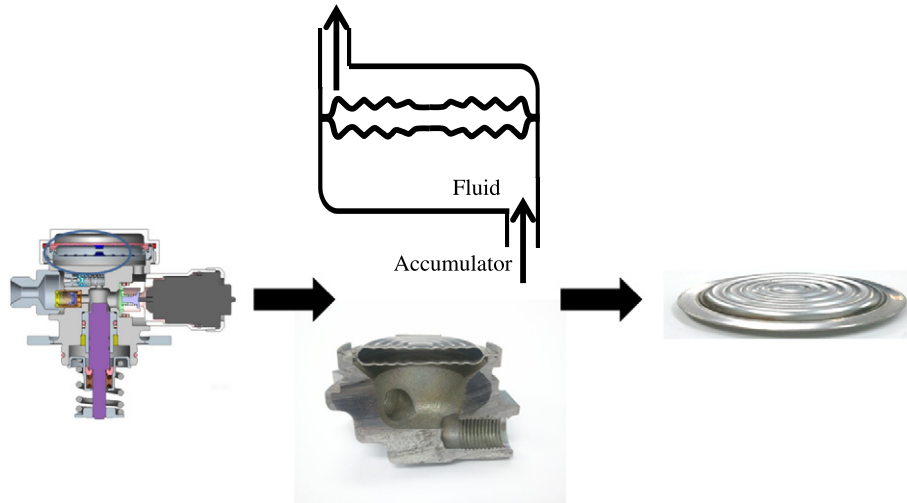


Fig. 2. Schematic of diaphragm-based pulsation damper (accumulator) and pumping module (material: SUS 316, tensile strength: 480 N/mm<sup>2</sup>).

## 2. Development of FE procedure for diaphragm-based pulsation damper simulation

This section describes the development of a new FE procedure that considers the fluid–gas–structure interaction to numerically estimate the performance of the diaphragm-based pulsation damper. We evaluate various factors including the damping fluid volume, resonance frequency, and von Mises stress.

### 2.1. Working principle of pulsation damper

The basic geometric dimensions of the cylindrical chamber in which the diaphragm-based pulsation damper is installed and operating conditions such as the operating pressures, angular speed of the engine, and flow directions were pre-determined by collaborating engineers at Motonic, Inc., which is developing a pump module for a GDI engine. Because mechanical components besides the pulsation damper were being developed simultaneously, we were unable to enlarge our design space or change the operating conditions of the pulsation damper. To explain the basic working principles of the damper in connection with those of the simple damper or accumulator shown in Fig. 1c, which is made of SUS 316, Fig. 2 (right) shows a schematic of the damper, which consists of a chamber and two metal diaphragms [5,16,17]. Gas (He) is supplied to the space between the two envelope-shaped diaphragms, causing the polytropic constant to become approximately 1.4. The gasoline flows back and forth through the small holes around the diaphragms. As noted in the Introduction, the working principle for this complex manifold damper is the same as that of the damper shown in Fig. 1c, except that the stiffness values of the metallic diaphragms must be considered [16,17].

To the best of our knowledge, three engineering factors play important roles when developing a diaphragm-based pulsation damper: the damping fluid volume, working frequency, and von Mises stress. Other factors such as the structural safety and sealing should also be considered, but these are beyond the scope of this research project. The damping fluid volume defines how much fluctuating fluid volume a pulsation damper can attenuate. The resonance frequency indicates the specific frequency at which a pulsation damper is most effective. Finally, the von Mises stress should be considered from a structural safety point of view. Because the fuel pump module, with its damper, is one of the key modules in a car, the structural safety, i.e., static failure and dy-

namic failure (fatigue), is much more important than the damping fluid volume and working frequency. To address all of these factors systematically, in this research, we develop an analysis tool based on a FE procedure that considers the simplified gas–fluid–structure interactions that occur.

#### 2.1.1. Damping fluid volume: determining basic pulsation damper size

From a power reserve point of view, the macroscopic relationship between the pressure and volume inside the pulsation damper, assuming an isenthalpic process, is given as follows [6,18]:

$$p_0 V_0^k = p_1 V_1^k = p_2 V_2^k (k = 1.4 \text{ for He}) \quad (1)$$

where the initial pressure, low pressure with inflated diaphragms, and high pressure with contracted diaphragms are denoted by  $p_0$ ,  $p_1$ , and  $p_2$ , respectively. The volumes corresponding to these three pressures are denoted by  $V_0$ ,  $V_1$ , and  $V_2$ , respectively. The polytropic constant of the gas used to fill the space between the diaphragms, assuming an isenthalpic process, is denoted by  $k$ . By manipulating the above equation, we can obtain the following formulation for the change in volume,  $\Delta V$ , between  $V_1$  and  $V_2$ .

$$\Delta V = V_1 - V_2 \quad (2)$$

$$V_0 = \frac{\Delta V}{\left(\frac{p_0}{p_1}\right)^{1/k} - \left(\frac{p_0}{p_2}\right)^{1/k}} = \frac{\Delta V \left(\frac{p_1}{p_0}\right)^{1/k}}{1 - \left(\frac{p_1}{p_2}\right)^{1/k}} \quad (3)$$

$$\Delta V = V_0 \left( \left(\frac{p_0}{p_1}\right)^{1/k} - \left(\frac{p_0}{p_2}\right)^{1/k} \right) \quad (4)$$

By applying Eqs. (2)–(4), we can determine the basic dimensions of a pulsation damper for a given fuel flow.<sup>1</sup> In other words, the equations above imply that the initial volume (or geometric size) of an accumulator should be determined based on the size of the fluctuating fuel volume. In (4), when the fluctuating fuel volume becomes large, a pulsation damper with a large initial volume,  $V_0$ , must be installed. This requirement is quite reasonable from an engineering context. Furthermore, in these basic equations, we observe that the internal pressures,  $p_1$  and  $p_2$ , should be determined and the

<sup>1</sup> Because the wavelength of the fluid fuel is much larger than the dimensions of the accumulator of interest (i.e., a several m range vs. about 5 cm), it is valid to assume that a constant fluid pressure is applied to the surfaces of the pulsation damper.

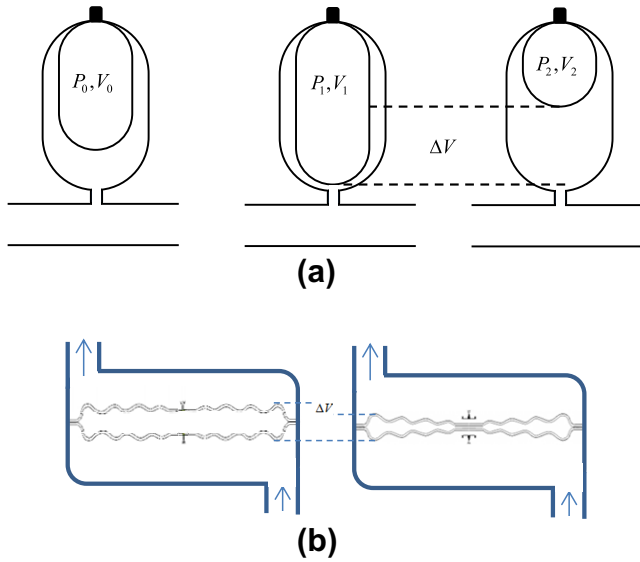


Fig. 3. Relationship between elementary damping fluid volume and real pulsation damper.

initial pressure,  $p_0$ , plays an important role [5,11,15,19]. If the stiffness values of the diaphragms or membranes separating the gas and gasoline could be neglected, the pressures  $p_1$  and  $p_2$  would be the same as those of the gasoline in the chamber or pipes, as shown in Fig. 3. However, in our pulsation damper, the membranes or diaphragms are made of metal. Therefore, their stiffness values cannot be neglected. Consequently, the engineering assumption that the pressures  $p_1$  and  $p_2$  are the same as those of the pipes is no longer valid. The internal pressures must be calculated while considering the stiffness effects of the diaphragms [8]. Thus, the next section describes the development of a new iterative FE procedure to calculate the internal pressures while considering the stiffness values of the elastic diaphragms. To the best of our knowledge, this problem has not previously been considered in the context of computational mechanics.

2.1.2. Resonance frequency

To understand the role of the resonance frequency, we first investigate the governing equation of a damper with the mem-

brane type shown in Fig. 4. Despite some differences in the flow direction, the geometry, gas pressures, and stiffness affect the developed metallic damper and existing rubber damper as shown in Fig. 4. They share the same working principles shown in Figs. 3 and 4. With approximations for the fluid, gas motion, and membrane, the basic governing equation becomes an ordinary simplified second-order differential equation. This governing equation is the same as that of the Helmholtz resonator [6,11,19]. For the sake of simplicity, the nomenclature is summarized in Fig. 4. The dynamic energy of the gasoline inside the pipes is most efficiently dissipated at the resonance angular speed by the gas packed inside the pulsation damper. Because we are concerned with gasoline (fluid) with a 1250 m/s wave speed, the resonance frequency ( $\omega_{resonance}$ ) of the pulsation damper calculated with the approximate physical parameters becomes relatively low, i.e., a few Hertz [6]. If one of the other types of dampers such as the Helmholtz resonator or T-filter in Fig. 1 is used, a very large damper (a few meters in size) should be used. Therefore, this diaphragm-based pulsation damper appears to be suitable for our application. As shown in Fig. 4, although the resonance frequency is an important characteristic, it is affected by the dimensions of other parts such as the pipe lengths and neck area. These dimensions are not the subject of our research.

2.1.3. Von Mises stress: static and dynamic failure

The fuel pump modules with diaphragm-based pulsation dampers used in commercial automotive applications must be structurally safe and reliable. Therefore, both static failure (yield) and dynamic failure (fatigue) should be considered. Because the pulsation damper is mainly under compressive fluid pressure, it is also reasonable to expect that the failure strength will improve. In our experimental setup, it was impossible to determine the dynamic failure characteristics [21]. Thus, in this research, because a commercially available diaphragm was shown to be strong enough in terms of static and dynamic failures, the von Mises stress of the diaphragm for an extreme pressure load is chosen to obtain a reference stress level by using a linear FE analysis.

2.2. FE procedure for damping fluid volume considering fluid-gas-structure interactions

As noted in the introduction, it is important to calculate the pressure of the internal volume by considering the volume change due to the fluid pressure load of gasoline. To the best of our

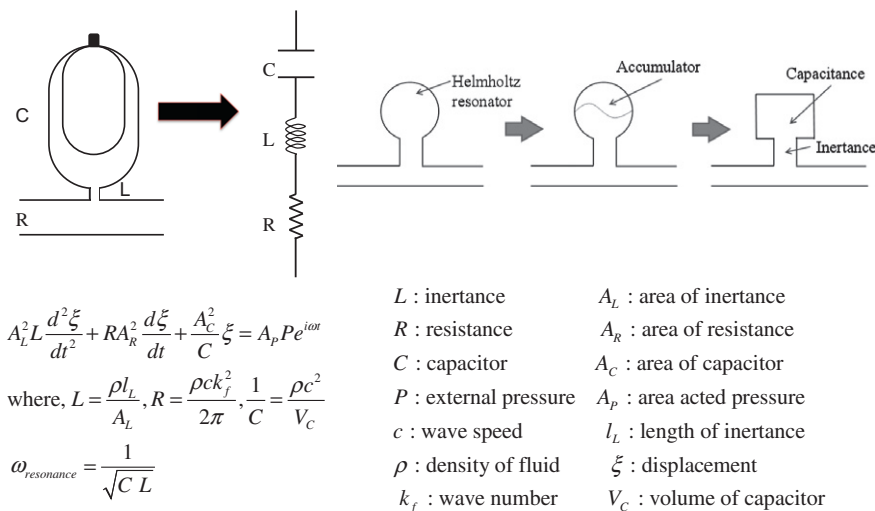


Fig. 4. Resonance frequency determination of diaphragm-based pulsation damper (See [6,20] for more detail).

knowledge, no commercial computational software exists for this purpose. Thus, in this subsection, we present a new FE procedure that considers the fluid–gas–structure interactions by addressing the following issues.

- FE issue 1: the identification of appropriate engineering assumptions to build a relatively accurate FE model that considers the mutual interactions among the fluid, gas, and structure.
- FE issue 2: the assessment of the FE accuracy of an asymmetric element versus three-dimensional element.
- FE issue 3: the development of an iterative procedure to update the locations of the nodes of the asymmetric FEs in order to calculate the inflated or contracted volume of the internal gas and the corresponding gas pressure.

2.2.1. Issue 1: engineering assumptions

We develop reasonable assumptions to build an accurate FE model that considers fluid–gas–structure interactions. First, we hypothesize that the domain of the metallic diaphragms can be modeled as a linear elastic structure without any difficulty. The pressure of the gasoline acts on the outside surfaces of the diaphragms, and the gasoline fills the outside area of the pulsation damper. Gas pressure also acts toward the internal surfaces of the diaphragms. To calculate the structural displacements of the diaphragms, the complex interactions among the fluid, gas, and structure must be considered. It may be possible to use the incompressible and compressible Navier–Stokes equations for the gasoline and gas domains, respectively. However, inevitably, a FE simulation becomes unnecessarily complicated, and the three different governing equations must be solved simultaneously. Thus, some engineering assumptions should be made. The wavelength and wave speed of gasoline (fluid) are more than 20 m and 1250 m/s, respectively. Therefore, in our opinion, it is valid to assume that the pressure variation along the outer surfaces of the diaphragms can be neglected. To calculate the gas pressure inside the diaphragms, we do not need to solve the compressible Navier–Stokes equation; rather, Eq. (1) can be used. Calculating the inflated or contracted inner volume of the pulsation damper while considering structural displacements is critical to the analysis. To

address this problem, we develop a new FE procedure, as shown in Fig. 5a, by combining geometric CAD operations.

2.2.2. Issue 2: accurate FE (axisymmetric versus three-dimensional element)

After comparing the accuracies in terms of the structural displacements and von Mises stresses of a three-dimensional FE model and axisymmetric FE model, we decided to use the axisymmetric FE implemented in ANSYS to estimate the damping fluid volume and mechanical stresses. The bending deflection of the diaphragms could not be properly estimated for three-dimensional tetrahedral or brick elements. The computational time required would also have been substantial. In contrast, the mechanical stresses of the diaphragms can be accurately obtained within a reasonable computation time by considering the axisymmetric element.

Nevertheless, the use of a two-dimensional axisymmetric element becomes another hurdle in calculating the internal three-dimensional volume of the expanded or contracted pulsation damper while considering its structural deformation. With a three-dimensional geometric model, geometric operators such as “volume subtract” and “volume add” can be used to easily calculate the volume inside the accumulator. However, it is difficult or impossible to perform this task using two-dimensional CAD and axisymmetric elements. To resolve this difficulty, we develop an in-house module to update the locations of the nodes of the axisymmetric elements of the diaphragms while first considering structural displacements. Then, we automatically draw spline lines that connect only the outer nodes (perimeter nodes) of the axisymmetric elements; the internal nodes do not need to be updated. By rotating the spline lines with the help of the geometric operators developed by ANSYS, we can build a three-dimensional volume model for inflated or contracted diaphragms. Next, a sufficiently large box is constructed and divided using the three-dimensional diaphragm model. By deleting the unnecessary volume, we can calculate the three-dimensional model inside the diaphragms and its volume with the help of the internal geometric operators from ANSYS. The procedures shown in Fig. 6 are developed using ANSYS and MATLAB.

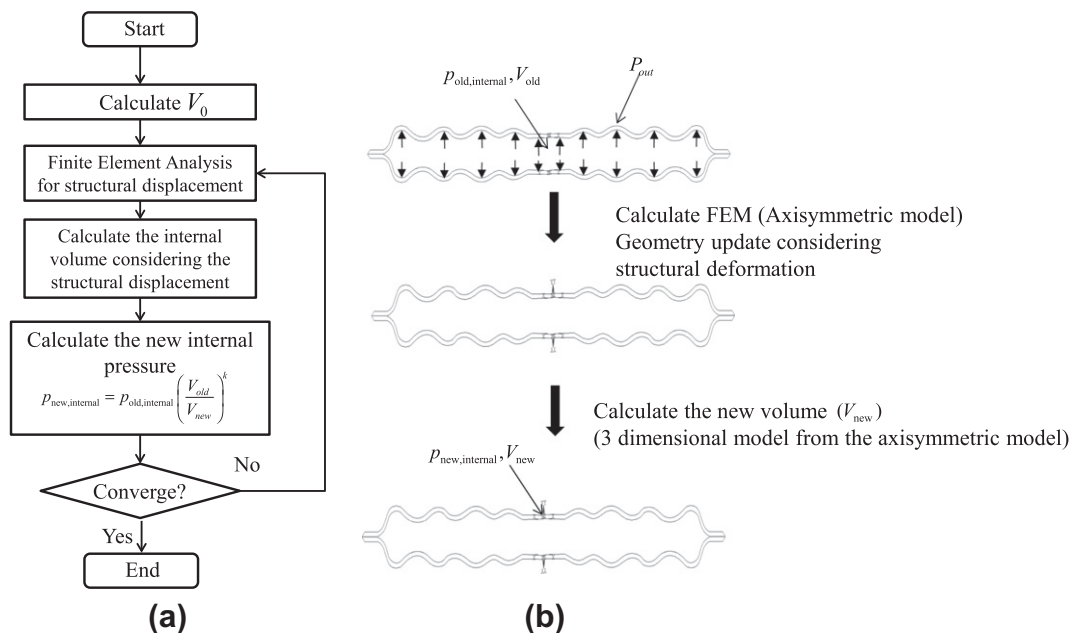


Fig. 5. FE procedure developed considering simplified fluid–gas–structure interactions.

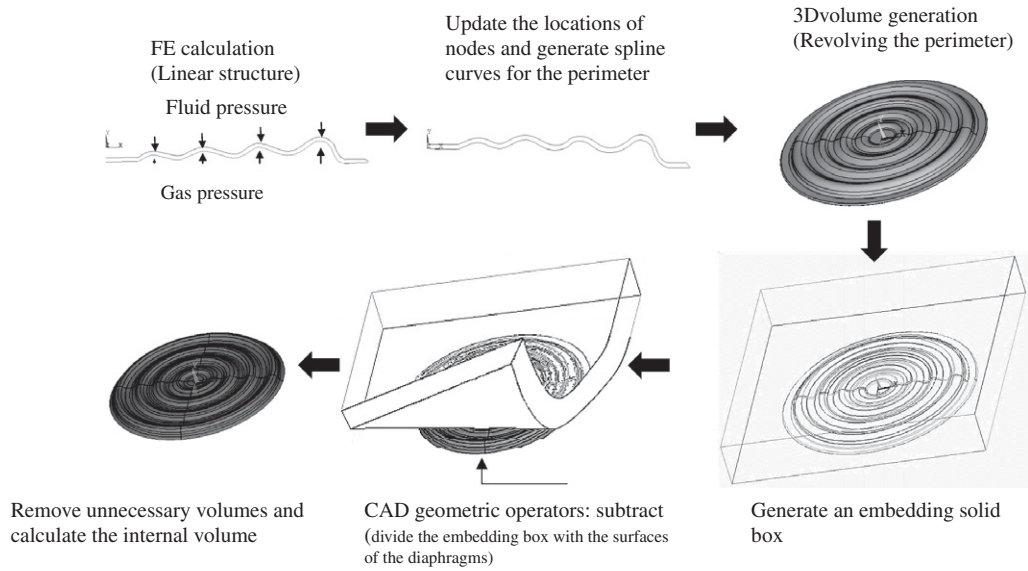
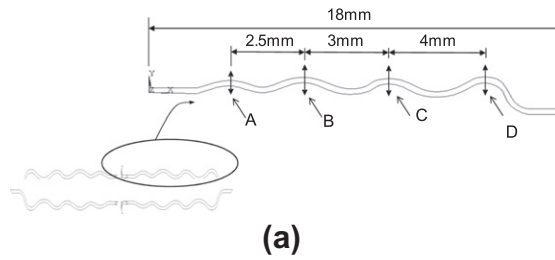


Fig. 6. Procedure used to calculate internal volume from two-dimensional axisymmetric FE model using CAD geometry operations.



(a)

| Run #<br>(Full factorial design) | Design matrix<br>(1: Decrease the height by -0.5 mm, 2: Maintain the current height, 3: Increase the height by +0.5 mm) |   |   |   |
|----------------------------------|---|---|---|---|
|                                  | A   | B | C | D |
| 1                                | 1   | 1 | 1 | 1 |
| 2                                | 1   | 2 | 2 | 2 |
| 3                                | 1   | 3 | 3 | 3 |
| 4                                | 2   | 1 | 2 | 3 |
| 5                                | 2   | 2 | 3 | 1 |
| 6                                | 2   | 3 | 1 | 2 |
| 7                                | 3   | 1 | 3 | 2 |
| 8                                | 3   | 2 | 1 | 3 |
| 9                                | 3   | 3 | 2 | 1 |

(b)

Fig. 7. Design variables chosen for diaphragms and DOE.

### 3. Optimal shape of diaphragm envelope found through design of experiments

In the previous section, an iterative FE procedure for assessing the performance of the accumulator while considering the fluid-gas-structure interactions was developed in the ANSYS framework. In this section, DOE is carried out in conjunction with the developed FE procedure.

The DOE method enables scientists and engineers to easily understand the individual and interactive effects of many design parameters from a structural point of view [21–25]. We use DOE to determine the optimal profiles for the diaphragm. Because of the symmetry of the section designs, only a quarter of the diaphragm is considered in Fig. 7. Future research may consider asymmetric designs for better performance. The design of the commercially available diaphragm that is currently used has four

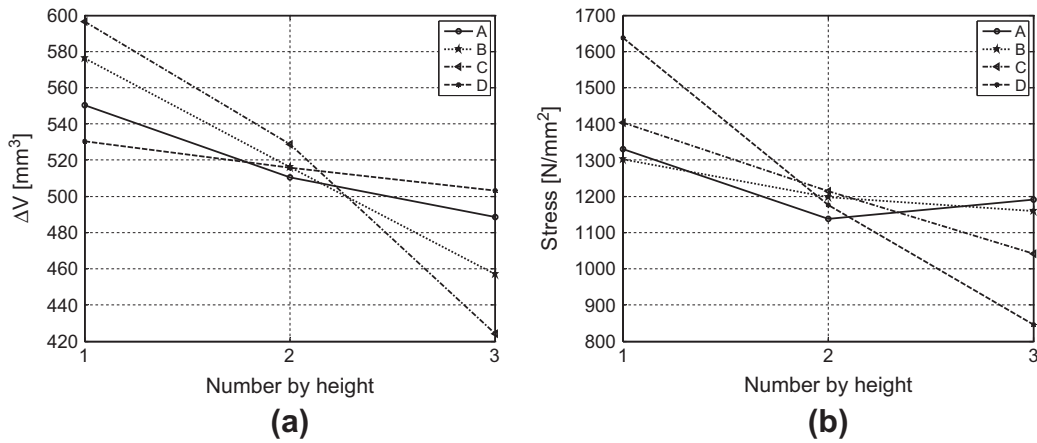


Fig. 8. Calculated damping fluid volume and von Mises stress for orthogonal array.

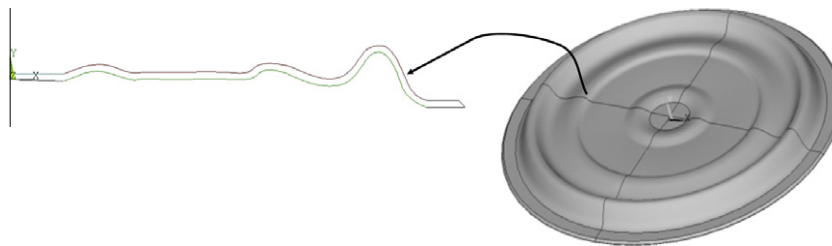


Fig. 9. Optimized designs from DOE.

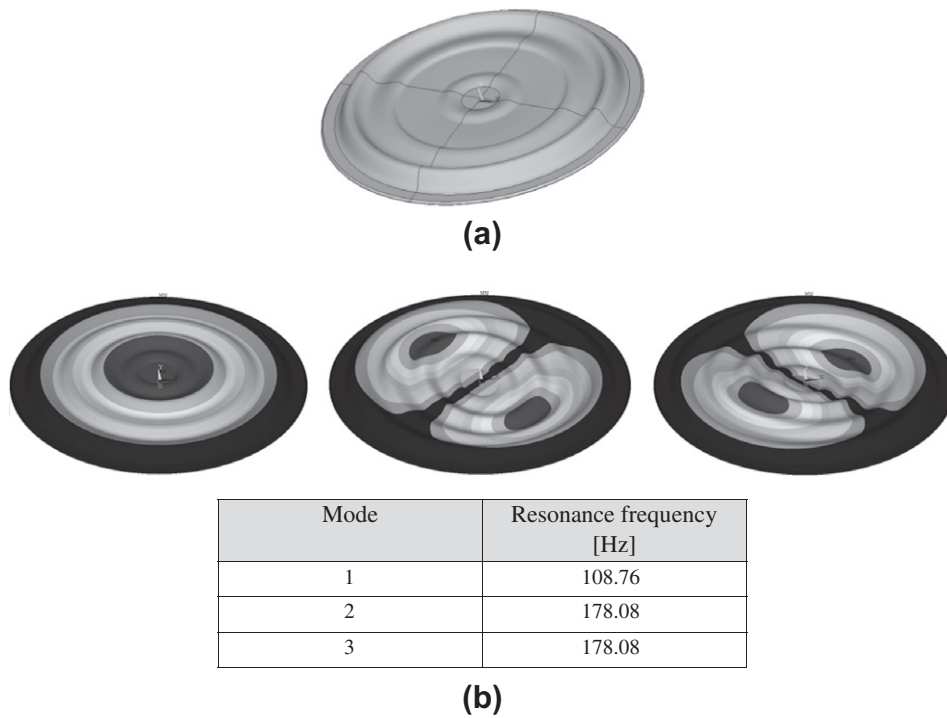


Fig. 10. Final shapes of diaphragms and associated eigenvalues without considering coupling with fluid.

waves, as shown in Fig. 7. The four parameters that represent the heights of these waves were optimized using DOE but are not presented in this paper. The damping fluid volume and von Mises stress are considered as performance measures. Therefore, the following objectives are pursued in this research.

$$\Delta V \geq \Delta V_{\text{Current}} \text{ and } \sigma_{\text{Von}}^{\text{Current}} \geq \sigma_{\text{Von}} \quad (5)$$

where the damping fluid volume and maximum von Mises stress of an existing diaphragm are denoted by  $\Delta V_{\text{Current}}$  and  $\sigma_{\text{Von}}^{\text{Current}}$ , respectively. The calculated damping fluid volume and maximum von

|                                       |   |
|---------------------------------------|---|
| Model                                 | Present diaphragm   |
| Design                                |  |
| Manufactured product                  |  |
| Diameter                              | Φ45.4 mm  |
| Thickness                             | 0.35 mm   |
| Gas                                   | He  |
| Internal pressure (Absolute pressure) | 10 bar  |

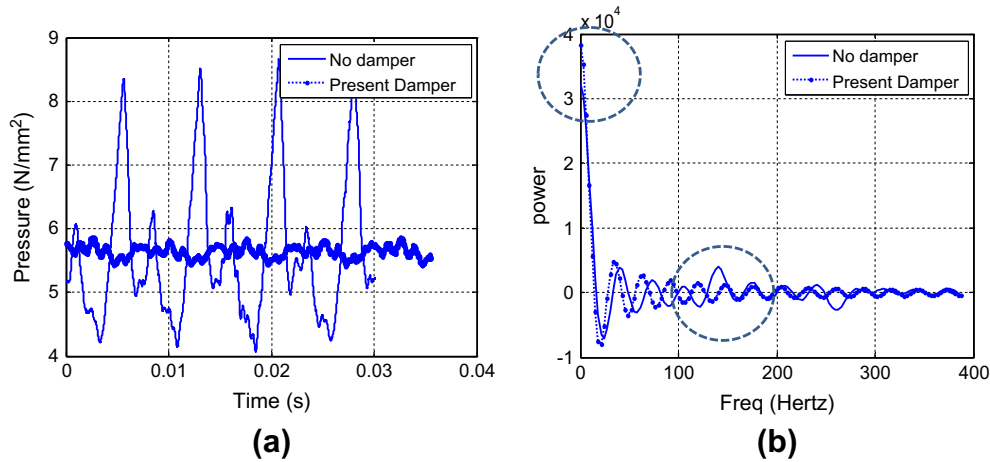
(a)



Fig. 11. (a) CAD model and diaphragm-based pulsation damper and (b) test bench installed by Motonic, Inc.

Mises stress of a modified design are denoted by  $\Delta V$  and  $\sigma_{von}$ , respectively. The objective of DOE is to maximize the damping fluid volume while minimizing the maximum von Mises stress. Because the frequencies of the oscillating fuel are much smaller than those of the diaphragms, they are not considered.

For clarity, the heights of the four waves are denoted by A, B, C, and D, and an APDL script is developed to automatically update the geometries of the diaphragm with updated parameters. The calculated damping fluid volume and von Mises stress for the DOE table shown in Fig. 7 are shown in Fig. 8. To conduct the DOE, the in-



**Fig. 12.** Experimental data (angular operating speed of motor: 2500 RPM): (a) time signal and (b) frequency response of signal (Hanning window for FFT).

creased or decreased y-step value for status 1 and status 2 is chosen to be 0.5 mm. This value is used because of the space limitation and the interference among the other parts of the pump. In addition to the y-position values of the waves, it is possible to conduct the DOE for the x-position values of the waves. The different effects of the design variables on these engineering factors are clearly observed as follows:

- Observation 1: From the perspective of the damping fluid volume, the effects of parameters C and B are significant, whereas the effect of parameter D is not significant.
- Observation 2: From the perspective of the von Mises stress, the effect of parameter D is significant, whereas the effects of parameters A and B are not significant. A larger value for parameter C will result in a smaller value for the von Mises stress.

Based on these observations, we conclude that parameter D can be decreased to lower the von Mises stress while maintaining the damping fluid volume. Furthermore, parameter B can be decreased to increase the damping fluid volume, by a slight increase in the von Mises stress. Based on these engineering observations, the parameters are manually updated as shown in Fig. 9b. The optimized design is shown in Fig. 9b. With the DOE procedure, it is possible to improve the damping fluid volume by 16.4% (from 523.2 mm<sup>3</sup> to 609.2 mm<sup>3</sup>) and to decrease the maximum von Mises stress by 0.71% (from 924.07 N/mm<sup>2</sup> to 917.49 N/mm<sup>2</sup>). The final CAD model, its eigenvalues, and its mode shapes are presented in Fig. 10 [7].

$$\begin{aligned} & \text{Max } \Delta V \\ & \text{subject to } \sigma_{\text{von}} - \sigma_{\text{von}}^{\text{Current}} \leq 0 \end{aligned} \quad (6)$$

#### 4. Manufacture and experimental testing

The test bench and pressure data measured for verification are presented in this section to demonstrate the performance of the optimized diaphragm design in terms of the damping fluid volume. Fig. 11 shows the CAD model, as well as the diaphragms and the test bench installed by Motonic, Inc. The pressure sensor (KISTLER, 4005B), AD converter, and Labview signal processing software are integrated in Fig. 11b. Because the directions of the flow inside the chamber are complex and arbitrary, unlike those of conventional accumulators, the pressure magnitudes of the input flow ahead of the GDI engine are directly measured using a pressure sensor, as shown in Fig. 12. A controllable pump is installed to generate

pressure oscillations. The Motonic engineers produced an operating environment that was conceptually similar to a car operating without an engine, as shown in Fig. 13a. The resulting pressure data and the graphs in the time and frequency domains are shown in Fig. 12. The magnitude of the pressure is significantly decreased and the average pressure is increased or compensated as a result of the pressure attenuation effect of the present pulsation damper, as shown in the circles. Furthermore, we show the alternating pressure with and without the damper for various angular speeds in Fig. 13a. As shown, the developed damper works well for various angular speeds. Furthermore, the effect of the internal pressure is shown in Fig. 13b. We cannot access the control method for the internal pressure because it is protected by another company. By decreasing the internal pressure, we can achieve better pressure attenuation.

#### 5. Conclusions

We optimized the y-direction profiles of the diaphragms used in a pulsation damper, which are key components of GDI engines in terms of structural safety and fuel efficiency. Because gasoline is directly injected into a GDI engine, high-pressure oscillation occurs inside the chamber and auxiliary pipes during the normal and idle operations. To reduce the magnitudes of these high-pressure oscillations, a diaphragm-based pulsation damper filled with helium gas is often installed ahead of a GDI engine. For fuel efficiency and structural safety, it is necessary to improve the pressure attenuation characteristics of the pulsation damper, including the damping fluid volume, resonance frequency, and von Mises stress. However, to the best of our knowledge, it is rare to conduct theoretical studies based on a coupled FE analysis to optimize this structure. Thus, this research developed an iterative FE procedure that simplifies the multiphysics phenomena among the elastic (or plastic) structure, fluid, and gas for a diaphragm-based pulsation damper and applied DOE to optimize the profile of the diaphragms.

Because the wavelength and wave speed of gasoline are high, we assumed that a uniform pressure at a magnitude that oscillates with respect to time was applied to the outsides of the diaphragms of interest. The pressure of the He gas inside the diaphragms could be calculated using a simple equation expressing the relationship between the volume and pressure, i.e.,  $pV^k = \text{constant}$ . To calculate the internal volume inside inflated or contracted diaphragms, we used an iterative procedure with axisymmetric FEs implemented in ANSYS. By updating the locations of the nodes while considering

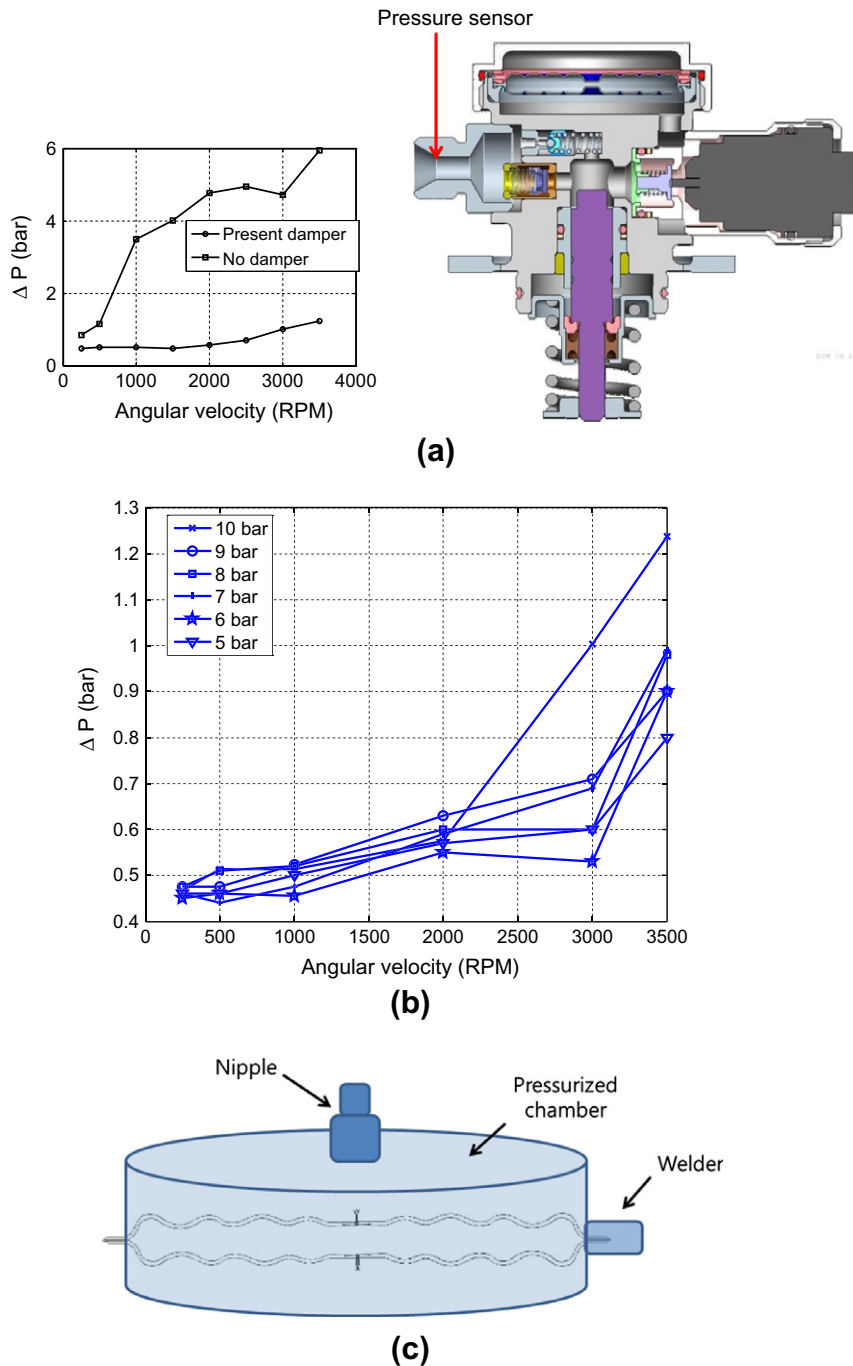


**Fig. 13.** Experimental data with respect to various angular speeds ( $\Delta p = \max(P) - \min(P)$ ): the averaged alternating pressure during 1 min of operation): (a) comparison without damper, (b) comparison of internal pressures, and (c) concept of manufacturing method.

structural displacements, creating a three-dimensional geometric model based on the updated nodes, and utilizing graphical operations, we could calculate the volume values of the inflated and contracted pulsation dampers. These values were used for calculating the corresponding internal pressure values. After an iterative FE procedure, the damping fluid volume and von Mises stress were calculated, and DOE was applied. This DOE procedure successfully determined the optimized profile of the diaphragms by maximizing the damping fluid volume while minimizing the maximum von Mises stress. To assess the damping efficiency of the developed module, the optimized pulsation damper module was manufactured with the help of an external

manufacturer and tested. Our experiments showed that the damping effect could be successfully obtained at lower frequency ranges. In future research, it may be possible to change the  $x$ -direction profile of the diaphragm and obtain better performance. Furthermore, some innovative manufacturing processes for the diaphragm-based pulsation damper filled with high-pressure gas should be developed.

In conclusion, after determining the working principle of the pulsation damper for GDI engines, an iterative FE procedure was developed to simulate the multidisciplinary fluid–gas–structure interactions, and DOE was applied to optimize the profiles of the diaphragms.

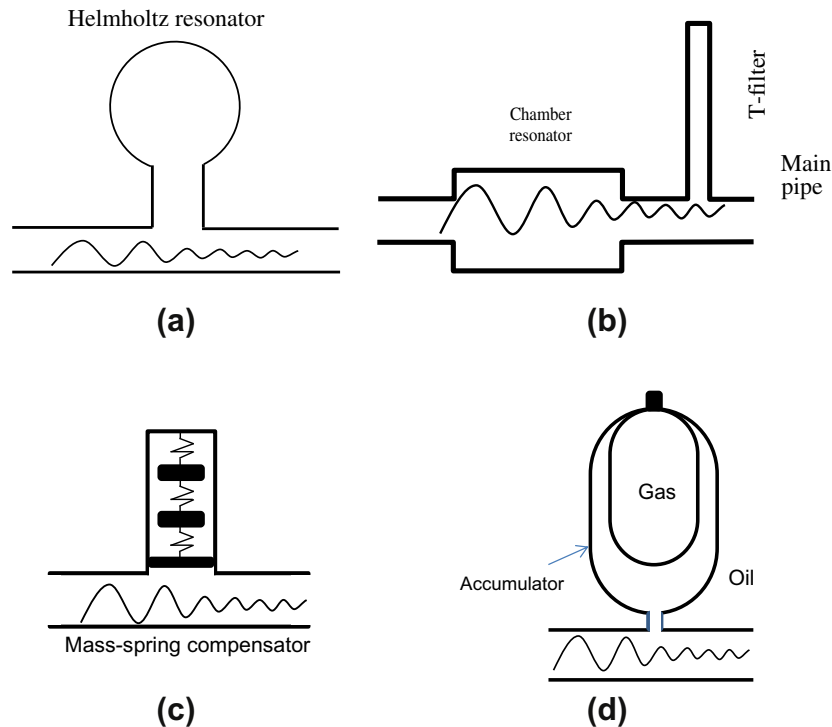


**Fig. 14.** Types of pulsation dampers: (a) Helmholtz resonator, (b) expansion chamber with T-filter, (c) mass-spring compensator, and (d) diaphragm-based pulsation damper [5,6].

## Acknowledgement

The authors acknowledge the support from Motonic Inc. and the National Research Foundation of Korea(NRF) grant funded by the Ministry of Education, Science and Technology (No. 2012R1A1A2A10038803)(GHY).

## Appendix A. Type of accumulator

There are many kinds of pressure or acoustic dampers, as shown in Fig. 14 [5,7,8], and many kinds of passive and active dampers have been developed [5,7,8]. The commonly implemented passive pulsation dampers, as shown in Figs. 14a–c, include the Helmholtz resonator, the expansion chamber resonator with a T-filter, and the mass-spring damper, respectively. These have been widely used in acoustic and fluid pressure attenuation. Fig. 14d shows a schematic of the pulsation damper, which has been commercialized for general purposes but is not suitable for automobile applications in its present form [11]. Because the separator between the gas and fluid is made of an elastic membrane such as rubber or plastic, the stiffness and strength of the diaphragm is too low to resist the high fluid pressure (around 10 bar) inside a GDI engine. With some changes, the pulsation damper under development, shown in Fig. 14d, may be a feasible solution. Although the dampers or accumulators in Fig. 14 look very different, they operate on the same governing principle for calculating pressure attenuation [5,6,11–15]. The choice among these pulsation dampers depends greatly on the sizes of the available geometric spaces and the frequency range of interest. To the best of our knowledge, the diaphragm-based pulsation damper in Fig. 14d is more effective at attenuating high-flow pressure fluctuation in a low frequency range than the other dampers [8]. As noted, high gasoline pressure fluctuation inside GDI engines is undesirable. It was the objective of the present research to develop a systematic engineering process for calculating the performance of the new pulsation damper numerically,

identifying the optimal characteristics for the pulsation damper, and verifying its performance experimentally.

## References

- [1] R Rotondi GB. Gasoline direct injection spray simulation. *Int J Thermal Sci* 2006;45:168–79.
- [2] Henriot S, Chaouche A, Cheve E, Duclos JM. CFD aided development of a SI-DI engine. *Oil Gas Sci Technol* 1999;54:279–86.
- [3] Ando H, Noma K, Iwamoto Y, Nakayama O, Yamauchi T. Development of gasoline direct injection (GDI) engine. *Jsm Int J C-Mech Sy* 1997;40:A15–6.
- [4] Brouzos NP. Experimental studies of CAI combustion in a four-stroke GDI engine with an air-assisted injector. In: School of engineering and design. Brunel University; 2007.
- [5] Wachel SMPJC. Understanding how pulsation accumulators work, pipeline engineering symposium, vol. 14; 1988 [Book No. 100256].
- [6] Kinsler LE. *Fundamentals of acoustics*. 4th ed. New York: Wiley; 2000.
- [7] Premnath RKPSSS. Resonant frequency analysis of the diaphragm in an automotive electric horn international ANSYS conf, vol. 121; 2006.
- [8] McEntee LB. Oscillating diaphragms. In: Proceedings of the international conference on modeling and simulation of microsystems, vol. 2; 1999. p. 597–600.
- [9] Ibrahim RA. Recent advances in nonlinear passive vibration isolators. *J Sound Vib* 2008;314:371–452.
- [10] Royston TJ, Singh R. Optimization of passive and active non-linear vibration mounting systems based on vibratory power transmission. *J Sound Vib* 1996;194:295–316.
- [11] Mlikota J. A Novel. *Compact Pulsation Compensator to Reduce Pressure Pulsations in Hydraulic Systems*. World Scientific; 2001.
- [12] Lee BJKUY, Lee JB, Sung CM, Lee US, Lee JS. Design optimization of an accumulator for noise reduction of rotary compressor. *Trans KSME* 2011;23:701–833.
- [13] Ijas TVM. Experimental study of hydraulic pulsation dampers for low frequencies. In: Sixth triennial international symposium on fluid control, measurement and visualization, sherbrook, flucome; 2000. p. 13–17.
- [14] Maillard J. Active control of pressure pulsations in piping systems. In: University of Karlskrona; 1998.
- [15] Sewall DAW John L, Herr Robert W. An investigation of hydraulic-line resonance and its attenuation. In: Center LR, editor. Langley research center; 1973.
- [16] Emanuele Bertarelli RA, Bianchi Elena, Laganà Katia, Corigliano Alberto, Dubini Gabriele, Contro Roberto, A multi-physics framework for the geometric optimization of a diaphragm electrostatic micropump. *COMSOL International Conference*. Milano; 2009. p. 14–16.

- [17] Mikota RSJ. Solid body compensators for the filtering of fluid flow pulsations in hydraulic systems. *Mechatronics and Robotics'99*. TU Brno Czech Republic; 1999.
- [18] DeWitt DP, Incropera Frank P. *Introduction to heat transfer*. John Wiley & sons; 1990.
- [19] Lari K. Attenuating amplitude of pulsating pressure in a low-pressure hydraulic system by an adaptive Helmholtz resonator. *Oulun Yliopisto Acta Univ Ouluensis C Tech* 2010;354.
- [20] Watanabe T HA. Macromodel generation for hybrid systems consisting of electromagnetic systems and lumped RLC circuits based on model order reduction. *Ieice T Fund Electr* 2004;E87a:398–405.
- [21] Budynas RG, Nisbett JK. *Shigley's mechanical engineering design*. 9th ed. New York: McGraw-Hill; 2011.
- [22] Saeed Maghsoodloo GO, Jordan Victoria, Huang Chen-Hsiu. Strengths and limitations of taguchi's contributions to quality, manufacturing, and process engineering. *J Manuf Sys* 2004;23:73–126.
- [23] Das MN, Giri NC. *Design and analysis of experiments*. 2nd ed. New York: Wiley; 1986.
- [24] Mason RL, Gunst RF, Hess JL. *Statistical design and analysis of experiments: with applications to engineering and science*. 2nd ed. New York: J. Wiley; 2003.
- [25] Bechhofer RE, Santner TJ, Goldsman DM. *Design and analysis of experiments for statistical selection, screening, and multiple comparisons*. New York: Wiley; 1995.